

Manuscript version: Author's Accepted Manuscript

The version presented in WRAP is the author's accepted manuscript and may differ from the published version or Version of Record.

Persistent WRAP URL:

<http://wrap.warwick.ac.uk/145786>

How to cite:

Please refer to published version for the most recent bibliographic citation information. If a published version is known of, the repository item page linked to above, will contain details on accessing it.

Copyright and reuse:

The Warwick Research Archive Portal (WRAP) makes this work by researchers of the University of Warwick available open access under the following conditions.

© 2020 Elsevier. Licensed under the Creative Commons Attribution-NonCommercial-NoDerivatives 4.0 International <http://creativecommons.org/licenses/by-nc-nd/4.0/>.



Publisher's statement:

Please refer to the repository item page, publisher's statement section, for further information.

For more information, please contact the WRAP Team at: wrap@warwick.ac.uk.

1
2
3
4
5
6
7
8
9
10
11
12
13
14
15
16
17
18
19
20
21

A global model for flame pulsation frequency of buoyancy-controlled rectangular gas fuel fire with different boundaries

Xianjia Huang^a, Tao Huang^b, Xunjia Zhuo^b, Fei Tang ^{*,c}, Le He^b, Jennifer Wen^{*,d}

^a Joint Laboratory of Nuclear Power Plant Fire Safety, Institute of Industry Technology, Guangzhou & Chinese Academy of Sciences, Guangzhou 511458, China

^b State Key Laboratory of Nuclear Power Safety Monitoring Technology and Equipment, China Nuclear Power Engineering Co., Ltd, Shenzhen 518172, China

^c School of Automotive and Transportation Engineering, Hefei University of Technology, Hefei, Anhui 230009, China

^d School of Engineering, University of Warwick, Coventry CV4 7AL, UK

*Corresponding author:

Email address: Jennifer.wen@warwick.ac.uk

Postal address: School of Engineering, University of Warwick, Coventry CV4 7AL, UK

Email address: ftang@hfut.edu.cn;

Postal address: School of Automotive and Transportation Engineering, Hefei University of Technology, Hefei, Anhui, 230009, China

22 Abstract

23 Pulsation frequency is an important characteristic parameter for buoyancy-controlled fuel
24 diffusion flames. Fire experiments of a rectangular source with different aspect ratios were conducted
25 in an open space and against sidewalls made from a calcium silicate board. Due to the blocking effect
26 to restrict air entrainment to fire plumes, sidewall significantly reduced the flame pulsation frequency.
27 Furthermore, the effect of the fuel exit velocity on the pulsation frequency became intense as the aspect
28 ratio of the rectangle was increased to 7.45. Based on the modified hydraulic diameter for a rectangular
29 fire source with a sidewall and corner, a global model was developed for predicting the flame pulsation
30 frequency of the rectangular fire source with free, sidewall, and corner boundaries. The coefficient of
31 determination of this improved model is 0.9991, and the local errors of this model are less than 15%
32 considering all of the experimental data in the present work and available in the literature. This work
33 provides a method for predicting flame pulsation frequency, accounting for sidewall effect and aspect
34 ratio.

35

36 **Keywords:** Flame pulsation frequency; Rectangular fire source; Global model; Buoyancy-controlled
37 gas flame; Boundaries

38

39 1. Introduction

40 Rectangular fire sources are commonly used and have recently attracted considerable attention
41 from the research community. The flame height, centerline temperature and thermal radiation of a
42 flame generated by a rectangular fire source has been widely investigated [1-8]. The effect of
43 atmospheric pressure on the burning behavior of a rectangular fire source was studied numerically [9-
44 15]. Liu et al. [16] and He et al. [17] studied the interaction of two rectangular fires. Tang et al. [18]
45 investigated the maximum ceiling jet temperature generated by a rectangular-source fire in a tunnel.
46 Recently, Ji et al. [19, 20] and Zhang et al. [21] investigated the influence of sidewalls on the burning
47 behavior of a rectangular fire source; and found their effect to be of significance.

48 Generally, sidewalls next to fire exert blocking effect to restrict air entrainment to fire plumes. In
49 related studies, Zukoski et al. [22] found that the air entrainment of a fire source located against a
50 sidewall was reduced to 43% of that of a fire in an open space. Hasemi and Tokunaga [23] measured
51 the height of flame tips and continuous flames generated of wall fire. Poreh and Garrad [24]
52 investigated the flame height of wall and corner fire plumes and proposed two similar correlations to
53 estimate the effect of walls on the mean flame height were developed. Recently, several investigators
54 [19-21, 25-27] studied the influence of sidewalls on the burning behavior of pool fire. Hu et al. [28,
55 29] investigated the fire behavior of gas fires constrained by two parallel side walls and wall-attached
56 fire impinging upon an inclined ceiling. Tao et al. [30] investigated the flame characteristics of
57 buoyancy-controlled gas fire bounded by a sidewall and ceiling. Tang et al. [31,32] studied the fire
58 dynamics of the rectangular burner in a tunnel.

59 Flame pulsation is one of the basic characteristic parameters of pool fire [33, 34]. Malalasekera
60 et al. [35] reviewed the experimental technique and scaling relationships for buoyancy-controlled
61 flame pulsation. The hydrodynamic nature of flame puffing was set as the interplay of buoyancy and

62 fluid motion. Based on an analysis of experimental data on the frequency of pulsation in different
63 burners, the pulsation frequency of flame can be described by

64

$$65 \quad f = C_1(1/D)^{0.5} \quad (1)$$

66 where D is effective diameter of burner, m; C_1 is an experimentally determined coefficient with a value
67 of 1.5, 1.6, and 1.68 in the models proposed by Malalasekera et al. [35], Cetegen and Ahmed [36],
68 McCaffrey [37], respectively.

69 Recently, Zhang et al. [38] studied the flame pulsation frequencies of buoyant turbulent diffusion
70 flames under free, sidewall, and corner conditions. Based on the mirror approach, they proposed global
71 models of flame pulsation using the effective perimeter of the burner as the length scale for the fire
72 source under sidewall and corner conditions. These models can be expressed as [38]

73

$$74 \quad f = \begin{cases} 0.53 \sqrt{\frac{g}{D_{\text{eff}}}} & \text{free flames} \\ 0.52 \sqrt{\frac{g}{D_{\text{eff}}^*}} & \text{sidewall and corner flames} \end{cases} \quad (2)$$

75

76 where g is acceleration due to gravity, m/s^2 . The perimeter-equivalent diameter D_{eff} was developed for
77 the free flames. Furthermore, based on the mirror model, a modified perimeter-equivalent
78 diameter D_{eff}^* was applied for the models of the sidewall and corner flames. Based on the mirror
79 approach, the modified perimeter-equivalent diameter was expressed as [38]

80

81

$$D_{\text{eff}}^* = \begin{cases} \frac{2W+2L}{\pi} & \text{free flames} \\ \frac{4W+2L}{\pi} & \text{sidewall flames} \\ \frac{4W+4L}{\pi} & \text{corner flames} \end{cases} \quad (3)$$

82

83 where W and L is the width and length of the rectangular source, m. According to the expressions in
84 Eqs. (1)–(3), these models ignore the effects of the fuel flow rate on the flame pulsation frequency.

85 The fuel exit velocity has a small but finite effect on the pulsation frequency of axisymmetric fire
86 source [35, 36]. The magnitude of this effect has been found to be related to the burner diameter and
87 fuel flow [36]. Taking the burner diameter and fuel exit velocity into account, the relationship between
88 the Strouhal and Froude numbers was developed as [35]

89

90

$$St = 0.52(1/Fr)^{0.505} \quad (4)$$

91

92 The Strouhal number, St , is expressed as

93

94

$$St = fL/U \quad (5)$$

95

96 where L is the characteristic length of pool, m; and U is the gas velocity at the burner surface, m/s;

97 The Froude number, Fr , is expressed as

98

99

$$Fr = U^2/(gL) \quad (6)$$

100

101 where g is the gravitational acceleration, m/s^2 .

102 For a rectangular fire, Cetegen et al. [39] studied the pulsation of planar buoyant plumes of helium
103 and helium/air mixtures from a nozzle with different aspect ratios. Owing to the difference in mixing
104 rates and the strength of the local buoyancy flux, the correlation of the plume pulsation frequency for
105 planar plumes is different from that for axisymmetric plumes. The width of rectangular fire source was
106 considered to be the characteristic length scale for the pulsation frequency correlation. This correlation
107 can be expressed as [39]

108

$$109 \quad St_w = 0.55 Ri_w^{0.45} \quad (7)$$

110

111 where $St_w = fW/U$ and $Ri_w = (\Delta\rho/\rho_\infty)gW/U^2$. $\Delta\rho$ is characteristic density difference, kg/m^3 ; ρ_∞ is
112 ambient density, kg/m^3 ;

113 Tang et al. [40] and Tu et al. [10] studied the effect of low air pressure on the flame pulsation
114 behavior of rectangular pool fires. The hydraulic diameter was introduced as the characteristic length
115 scale for the rectangular flame pulsation frequency correlation and can be expressed as [40]

116

$$117 \quad D_{hyd} = \frac{2LW}{L+W} \quad (8)$$

118

119 Then, the following flame pulsation frequency model for hydrocarbon pool fires was developed [40]:

120

$$121 \quad St_{hyd} = 0.86 Fr_{hyd}^{-0.5} \quad (9)$$

122

123 where $St_{hyd} = fD_{hyd}/U$ and $Fr_{hyd} = U^2/gD_{hyd}$. Eq. (9) was derived based on the experimental data
124 obtained using a rectangular fire in an open space.

125 The approaches regarding the flame pulsation of a rectangular fire source drawn by Cetegen et al.
126 [39] and Tang et al. [40] appear to be conflicting. Cetegen et al. [39] considered the width of a
127 rectangular fire source as the characteristic length for the flame pulsation frequency model, while Tang
128 et al. [40] used the hydraulic length. Furthermore, the sidewall effect on the flame pulsation frequency
129 was not investigated in these studies. Hence, the applicability of these models to a rectangular fire
130 source with a sidewall is unknown.

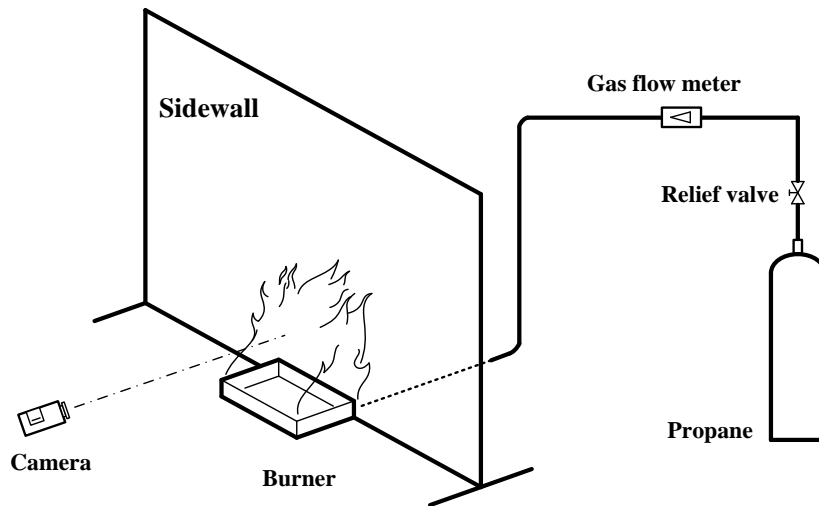
131 The present study focuses on the effect of sidewalls on the flame pulsation behavior of a
132 rectangular fire source with different aspect ratios. Fire experiments with rectangular burners of the
133 same surface area but different aspect ratios were conducted against a CS (calcium silicate) board. For
134 comparison, similar fire experiments were conducted with the same rectangular fire source without a
135 sidewall. The influence of sidewall and aspect ratios on the magnitude and frequency of flame
136 pulsation was discussed. Furthermore, based on the experimental data in present work and available
137 in the literature, a global model for predicting the frequency of flame pulsation was developed for a
138 rectangular fire in free, sidewall, and corner boundaries.

139

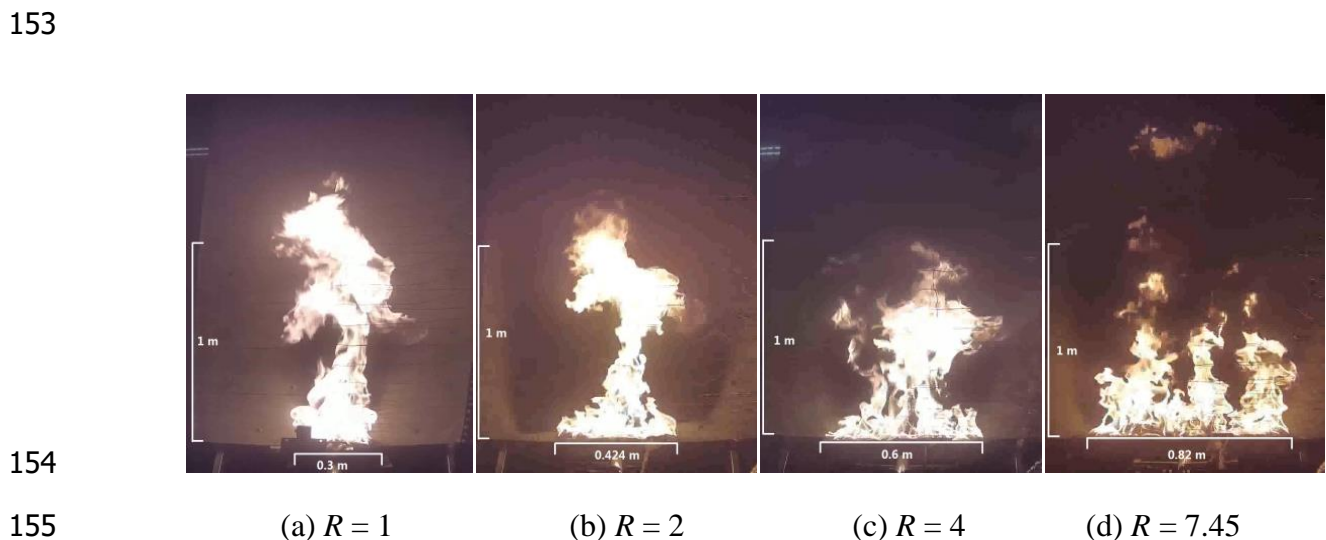
140 2. Experimental method

141 The schematic of the experimental setup is shown in Fig. 1. Propane was used as the fuel. Fire tests
142 were performed using one square, and three rectangular burners. The fire source was located against
143 the sidewall and there was no space between them. Fig. 2 shows the flame morphology of a rectangular
144 fire source located against a CS board ($\dot{Q} = 84.8$ kW). Fig. 3 presents sequential flame images taken
145 from the side of a rectangular fire located against a CS board at time intervals of 0.08 s ($R = 7.45$, $\dot{Q} =$

146 84.8 kW). All the burners had the same surface area but different aspect ratios. The burning surface
147 areas were 900 cm² for all the burners. The details of the tested scenarios are listed in Table 1. The
148 thermal properties and dimensions of the CS board used as sidewalls are listed in Table 2. Each fire
149 test was repeated two times to check repeatability. The tests were conducted in quiescent conditions
150 with wind speed being zero.



151
152 Fig. 1 Schematic of experimental setup



154
155 (a) $R = 1$ (b) $R = 2$ (c) $R = 4$ (d) $R = 7.45$
156 Fig. 2 Flame morphology of a rectangular fire source located against a CS board ($\dot{Q} = 84.8$ kW)

157 [27]

158



159

160 Fig. 3 Sequential flame images taken from the side of a rectangular fire located against a CS board at
 161 time intervals of 0.08 s ($R = 7.45$, $\dot{Q} = 84.8$ kW)

162

163

Table 1 Summary of fire scenarios

Burner shape	Surface area (cm ²)	Burner		Aspect ratio R	Heat release rate \dot{Q} (kW)
		Length (cm)	Width (cm)		
Square	900	30.0	30.0	1	28.3; 42.4; 56.5;
Rectangular	900	42.4	21.2	2	70.7; 84.8
Rectangular	900	60.0	15.0	4	
Rectangular	900	82.0	11.0	7.4	

164

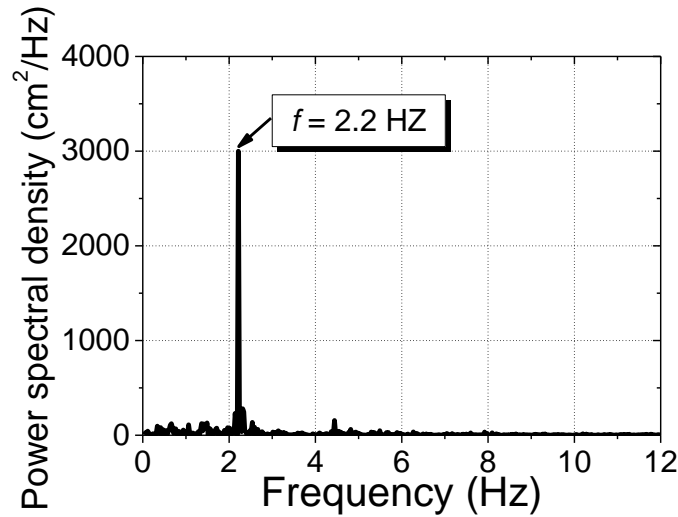
165

Table 2 Thermal properties of CS board

Materials	Density (kg/m ³)	Conductivity (W/mK)	Sp. ht. cap. (kJ/kgK)	Length (m)	Width (m)	Thickness (m)
calcium silicate	925	0.15	1.0	2.44	1.22	0.008

166

167 The flame shape was recorded using a digital CCD (Charge Coupled Device) camera (2592×1944
 168 pixels) with a film of 25 frames/s. The binary image processing technology captures the flame shape
 169 and converts it into binary images. It first calculates the height of the flame in the binary image, and
 170 then converts it into real height. Based on continuous images of the transient flame height, the flame
 171 pulsation frequency was deduced by the Fast Fourier Transform method [41]. Fig. 4 presents the flame
 172 pulsation frequency of a square burner ($R = 1$, $\dot{Q} = 84.8$ kW).



173

174

Fig. 4 Flame pulsation frequency of a square burner ($R = 1$, $\dot{Q} = 84.8$ kW)

175

176

177

178

179

180

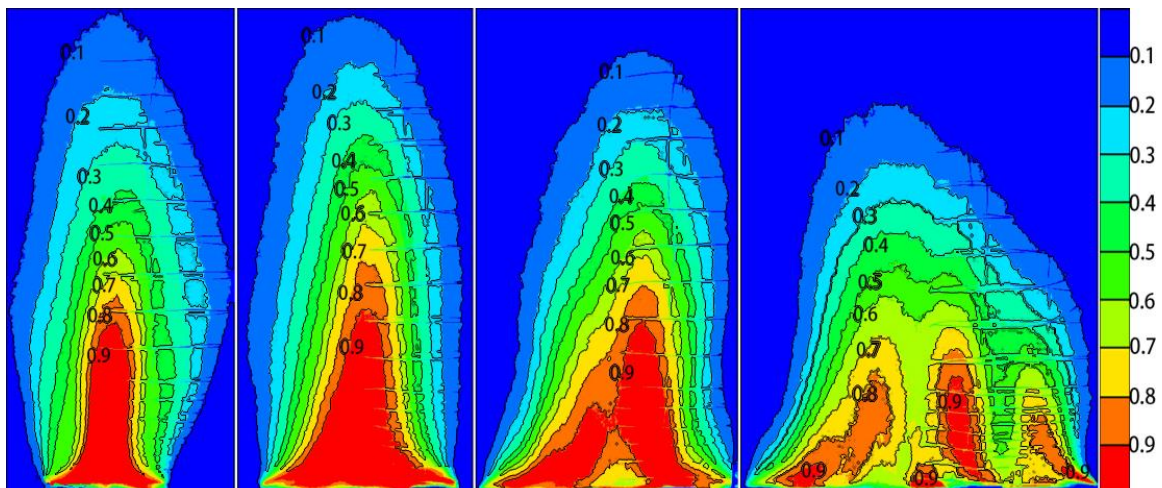
181

182

183

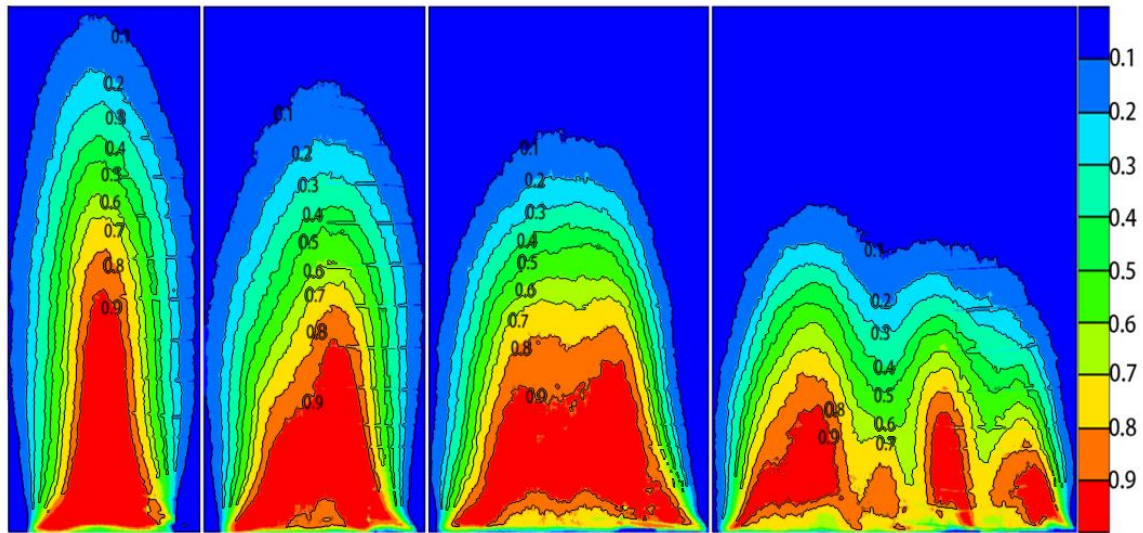
Figures 5 and 6 plot the contour image of flame height frequency for the rectangular fire source with a sidewall and in an open space, respectively. The flame diverged into several branches when the aspect ratio was increased to 7.45. This was in line with the observation in [6, 10]. It is likely that different air entrainment rates at different directions affected the local burning rates and flame shapes. As the length of the burner became longer than its width, more air was entrained from the length of burner. For a small section of rectangular fire source, the ratio of air to fuel increased with better air and fuel mixing. As the width of burner became smaller, the fuel flow injected from the burner was easier to be separated to give more sub-flames.

184



185 (a) R = 1 (b) R = 2 (c) R = 4 (d) R = 7.45

186 Fig. 5 Contour image of flame height frequency for the rectangular fire source with different aspect
187 ratios against the CS board.



188
189 (a) R=1 (b) R=2 (c) R=4 (d) R=7.45

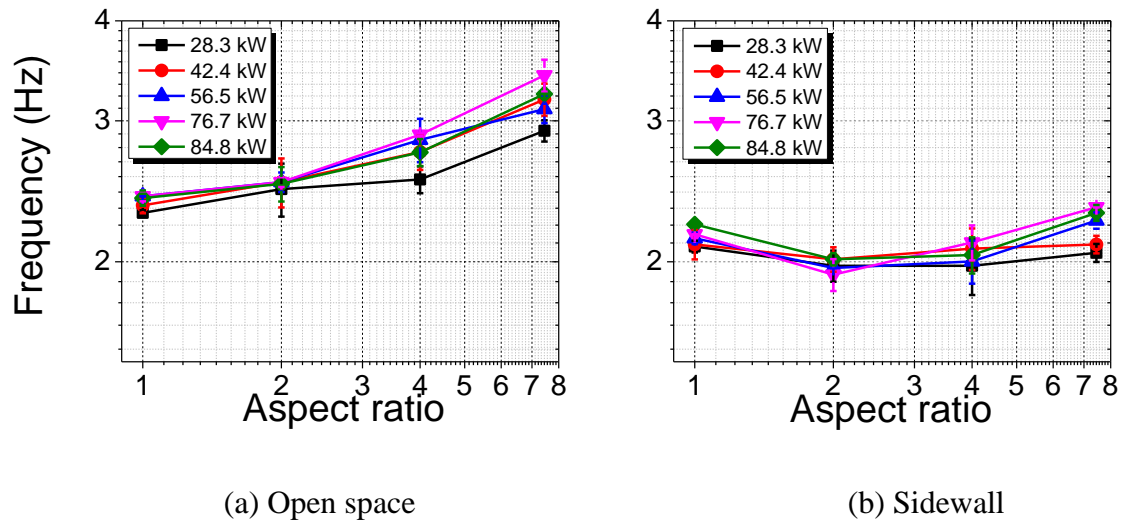
190 Fig. 6 Contour image of flame height frequency for the rectangular fire source with different
191 aspect ratios in the open space ($\dot{Q} = 84.8$ kW).

192 3. Flame pulsation frequency

193 Figure 7 shows flame pulsation frequency of rectangular fire with different boundary conditions.
194 Flame pulsation frequency is deduced from the variation of flame height. For the rectangular fire
195 without the sidewall, flame pulsation frequency increased in a linear manner with the increase in aspect
196 ratio. This was the same conclusion reached by Tu et al. [10] and Tang et al. [40]. As the fire source
197 was located against a sidewall, the flame pulsation frequency decreased significantly. This was within
198 1.9 - 2.3 Hz as the aspect ratio increased from 1 to 7.45.

199 The effect of the fuel exit velocity on the pulsation frequency became intense as the aspect ratio
200 of the rectangular burner became larger than 2 for fire source in the open space and 4 for fire source
201 against the sidewall, as shown in Table 3. For the rectangular fire source in the open space, as the heat

202 release rate increases, the maximum growth rate of the flame pulsation frequency is 13.7% and 17.3%
 203 for aspect ratios of 4 and 7.45, respectively. When the fire source was located against the sidewall, the
 204 maximum growth rate of the flame pulsation frequency increased suddenly from 7.0% to 14% as the
 205 aspect ratio was increased from 4 to 7.45. Therefore, the fuel exit velocity should be taken into account
 206 in the pulsation frequency model, especially for a rectangular fire source with a high aspect ratio.



209 Fig. 7 Flame pulsation frequency of rectangular fire with different boundary conditions.

210
211 Table 3 Maximum growth rate of flame pulsation frequency

	Open space	Sidewall
RN1	4.9%	6.6%
RN2	0.5%	4.5%
RN4	13.7%	7.0%
RN7.45	17.3%	14%

212

213 4. A global model of flame pulsation frequency

214 According to previous studies [38-40], the burner width [39], perimeter-effective diameter [38],
 215 and hydraulic diameter [40] can be used as the characteristic length for the flame pulsation frequency
 216 model in an open space. For a rectangular fire source with a sidewall, the burner width cannot

217 differentiate a rectangular fire source in an open space from the one with a sidewall. Thus, the
218 perimeter-effective diameter and hydraulic diameter were used for the global flame pulsation
219 frequency correlation under free, sidewall, and corner conditions.

220 The hydraulic diameter is considered as more suitable characteristic parameter for the pulsation
221 frequency than the perimeter-effective diameter. The perimeter-effective diameter indicates the
222 contact area of flame surface with stagnant surroundings. While the hydraulic diameter is mainly used
223 for calculations involving turbulent flow. Based on the conclusion in [36], the pulsation frequency was
224 found to be closely connected with the convection within one diameter height above the fire source.
225 The convection between the buoyant plume gas and the stagnant surroundings was turbulent flow and
226 reduced by the sidewall and the corner. Therefore, the hydraulic diameter can be used as correlation
227 for the pulsation frequency.

228 For a rectangular fire source with free, sidewall and corner boundaries, the expression of
229 hydraulic diameter for the global pulsation model is

230

$$231 \quad D_{\text{hyd}} = \begin{cases} \frac{4LW}{2(L+W)} & \text{free flames} \\ \frac{4LW}{2W+L} & \text{sidewall flames} \\ \frac{4LW}{L+W} & \text{corner flames} \end{cases} \quad (10)$$

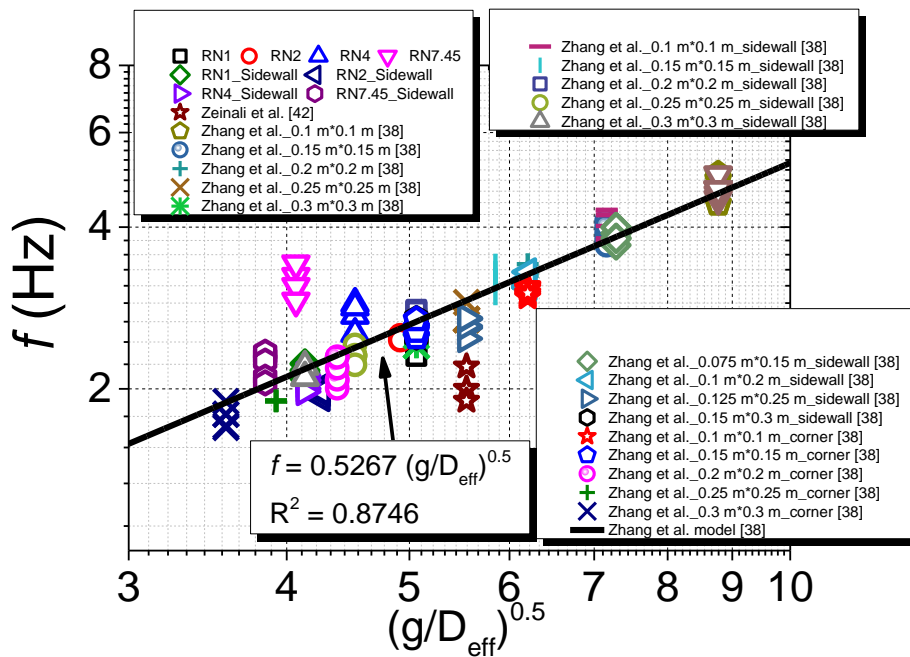
232

233 According to the assumption of the mirror model [38], the expression for the hydraulic diameter does
234 not change if the mirror model is applied for sidewall and corner flames. The expressions of the
235 perimeter-equivalent diameter for fire sources with different boundaries are shown in Eq. (3).

236 Figure 8 shows the global flame pulsation frequency correlation based on the perimeter-
237 equivalent diameter. The fitted correlation is almost the same as that of the model proposed by Zhang

238 et al. [38] (Eq. (2)). The coefficient of determination is only 0.8746. As the fuel flow rate is ignored,
 239 this global correlation has low accuracy in estimating the experimental data of rectangular burners
 240 with large aspect ratios (4 and 7.45). Furthermore, this global correlation over-estimates the flame
 241 pulsation frequency of the fire source in the corner, which can be proved by the experimental data
 242 from Zeinali et al. [42].

243



244

245 Fig. 8 Global flame pulsation frequency correlation based on the perimeter-equivalent diameter.

246

247 Based on the experimental results in present work and data available in the literature [38, 42], the
 248 global flame pulsation frequency correlation based on dimensionless parameters (Strouhal number and
 249 Froude number) with perimeter-equivalent diameter is fitted as

250

251

$$St = 0.71 Fr_{eff}^{-0.48} \quad (11)$$

252

253 Global correlation of flame pulsation frequency based on dimensionless parameters (Strouhal number
254 and Froude number) with hydraulic diameter is expressed as

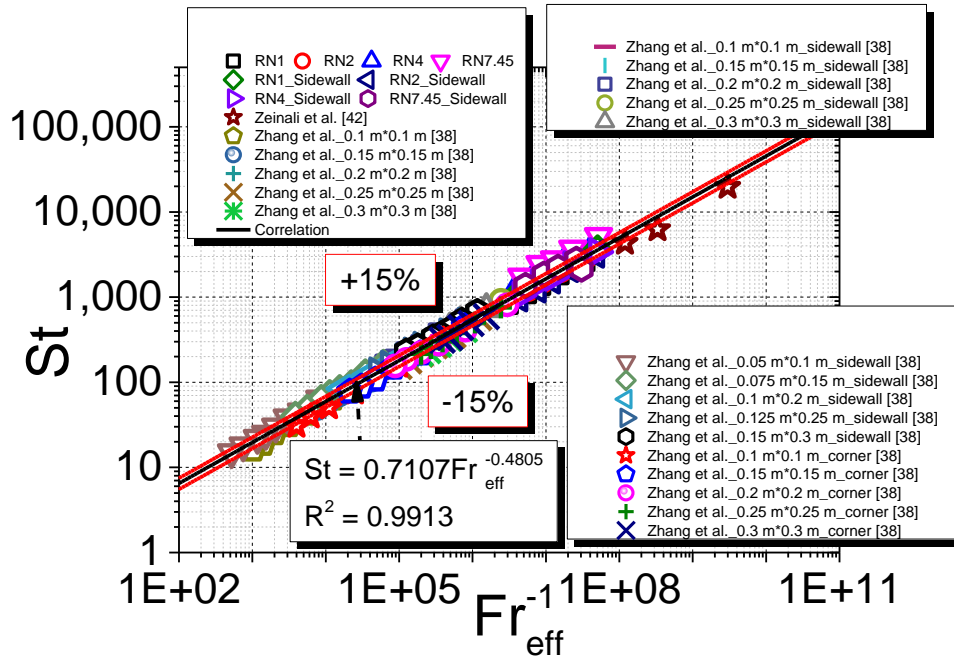
255

$$256 \quad St = 0.53 Fr_{\text{hyd}}^{-0.49} \quad (12)$$

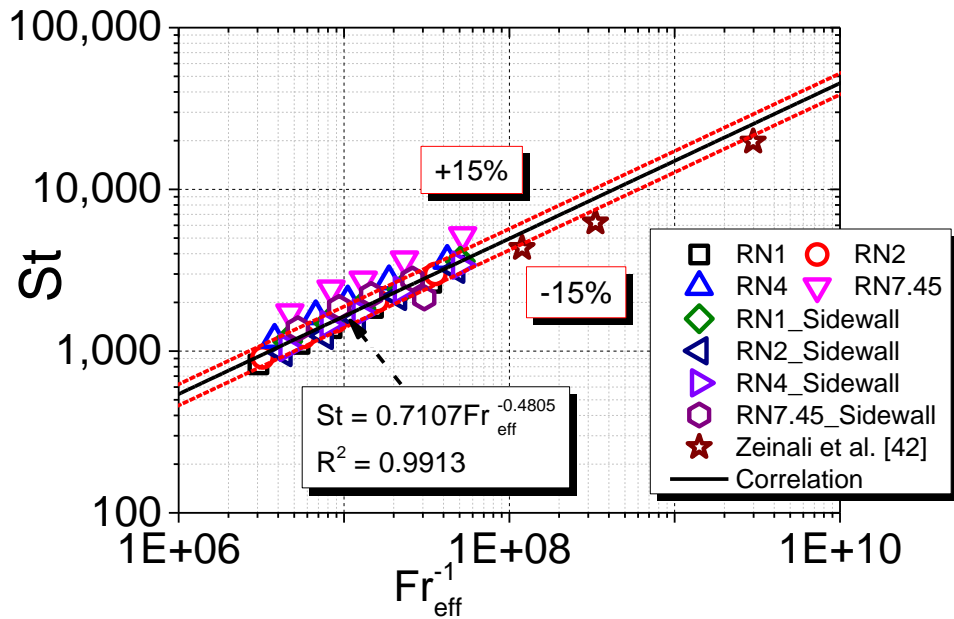
257

258 Figures 9 and 10 show the global flame pulsation frequency correlations based on dimensionless
259 parameters (Strouhal and Froude numbers) with the perimeter-equivalent diameter and hydraulic
260 diameter, respectively. The global flame pulsation frequency correlation with the hydraulic diameter
261 has better accuracy than that with the perimeter-equivalent diameter. Even though the coefficients of
262 determination for these two global correlations are both greater than 0.99, the global correlation with
263 the perimeter-equivalent diameter performed poorly for the rectangular fire source with an aspect ratio
264 of 7.45 and the fire source in the corner. In this case, the local errors of the correlation are larger than
265 15%, as shown in Fig. 9(b). However, the local errors of the global correlation with hydraulic diameter
266 for all the fire tests are less than 15%, as shown in Fig. 10. Evidently, the hydraulic diameter is a better
267 characteristic length for the global flame pulsation frequency model.

268

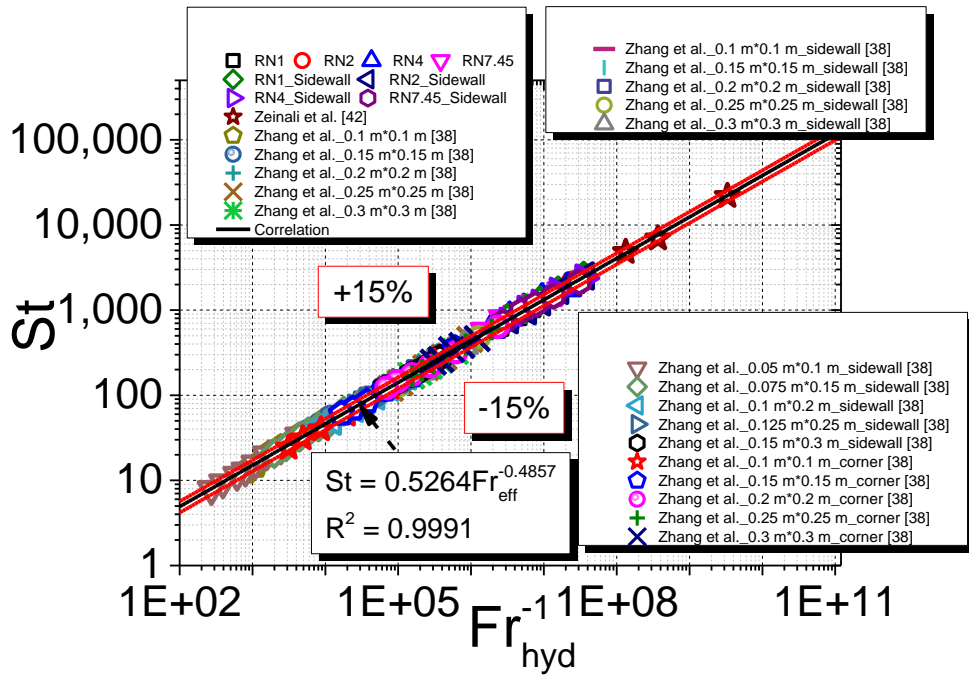


(a) All data



(b) Data from the present work and Zeinali et al. [42]

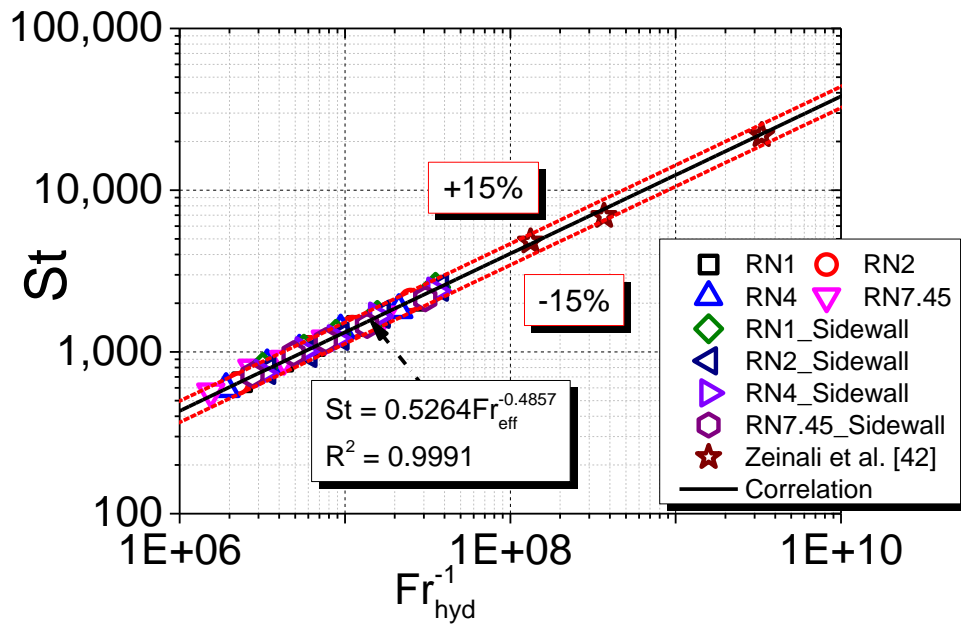
Fig. 9 Global flame pulsation frequency correlation based on dimensionless parameters (Strouhal number and Froude number) with perimeter-equivalent diameter.



276

277

(a) All data



278

279

(b) Data from the present work and Zeinali et al. [42]

280 Fig. 10 Global correlation of flame pulsation frequency based on dimensionless parameters (Strouhal

281

number and Froude number) with hydraulic diameter.

282

283 5. Conclusions

284 This study focuses on the flame pulsation frequency of the rectangular fire with different
285 boundaries. Rectangular fire experiments were conducted in an open space and with a CS board. The
286 presence of a sidewall has significant effect on the flame pulsation behaviors of a rectangular fire
287 source. The blockage of air entrainment by the sidewall significantly reduced frequency of flame
288 pulsation. Furthermore, the effect of the fuel exit velocity on the pulsation frequency should be taken
289 into account for the pulsation frequencies of rectangular fire sources with high aspect ratios.

290 A global correlation was developed for the frequency of flame pulsation generated by the
291 rectangular fire source with different boundaries. The hydraulic diameter of the rectangular fire source
292 was modified for the characteristic parameter for the global frequency model of flame pulsation. Then,
293 based on the experimental data obtained in the present work and available in the literature, a global
294 model for puffing frequency was improved for the rectangular fire source with free, sidewall, and
295 corner boundaries. The coefficient of determination of this model is 0.9991 and the local error of this
296 fitted correlation was less than 15%, which show that the experimental data can be expressed quite
297 accurately with this correlation. Compared with the perimeter-effective diameter, the hydraulic
298 diameter is a better characteristic length scale for the flame pulsation frequency correlation of the
299 burner with different boundaries.

300 The flame pulsation frequency was determined by the convection between the buoyant plume gas
301 and stagnant surroundings. The perimeter-effective diameter indicates the contact area of the flame
302 surface with the stagnant surroundings and ignores the turbulence flow of the gas flame. The hydraulic
303 diameter used for calculations involving turbulent flow more accurately describes the correlation of
304 the flame pulsation frequency than the perimeter-effective diameter.

305

306

307 **Acknowledgements**

308 The work presented in this paper is supported by the National Key Research and Development
309 Program of China (Project No. 2016YFC0800100); National Nature Science Funds of China under
310 Grant No. 52076066; Guangzhou Science and Technology Plan Program of China (Project No.
311 202002030124), and National Nature Science Funds of China under Grant No. 51776060.

312

313 **References**

- 314 [1] Y Hasemi, M Nishihata. Fuel shape effect on the deterministic properties of turbulent diffusion
315 flames, *Fire Saf. Sci.* 1987; 7:227-234. https://doi.org/10.11196/kasai.38.2_29
- 316 [2] JG Qunitiere, BS Grove. A unified analysis for fire plumes, *27th Symp. Combust. Inst.* 1988; 2757-
317 2766. [https://doi.org/10.1016/S0082-0784\(98\)80132-X](https://doi.org/10.1016/S0082-0784(98)80132-X)
- 318 [3] LH. Hu, XC. Zhang, XL. Zhang, LZ Yang. A re-examination of entrainment constant and an
319 explicit model for flame heights of rectangular jet fires, *Combust. Flame* 2014; 161:3000-3002.
320 <https://doi.org/10.1016/j.combustflame.2014.05.003>
- 321 [4] W Gao, NA Liu, Y Jiao, XD Xie, Y Pan, ZL Li, XS Luo, LH Zhang, R Tu. Flame length of buoyant
322 turbulent slot flame, *Proc. Combust. Inst.* 2019; 3:3851-3858.
323 <https://doi.org/10.1016/j.proci.2018.05.153>
- 324 [5] ZH Zhou, GH Chen, CL Zhou, CL Zhou, K Hu, Q Zhang. Experimental study on determination of
325 flame height and lift-off distance of rectangular source fuel jet fires, *Appl. Therm. Eng.* 2019;
326 152:430-436. <https://doi.org/10.1016/j.applthermaleng.2019.02.094>
- 327 [6] XJ Huang, XJ Zhuo, T Huang, ZM Zheng, CH Cheng, WK Chow. Simple flame height correlation
328 for buoyancy-controlled diffusion plumes generated by rectangular sources fire with different
329 aspect ratios, *FUEL*, 2019; 254:115655. <https://doi.org/10.1016/j.fuel.2019.115655>

- 330 [7] CG Gong, L Ding, HX Wan, J Ji, ZH Gao, LX Yu. Spatial temperature distribution of rectangular
331 n-heptane pool fires with different aspect ratios and heat fluxes received by adjacent horizontal
332 targets, *Fire Saf. J.* 2020; 112:102959. <https://doi.org/10.1016/j.firesaf.2020.102959>
- 333 [8] XJ Huang, XJ Zhuo, T Huang, CL Xing, CH Cheng, WK Chow. Thermal radiation model for the
334 buoyancy-controlled diffusion plumes from rectangular fire sources, *Int. J. Therm. Sci.*
335 2019;150:106234. <https://doi.org/10.1016/j.ijthermalsci.2019.106234>
- 336 [9] LH Hu, F Tang, Q Wang, ZW Qiu. Burning characteristics of conduction-controlled rectangular
337 hydrocarbon pool fires in a reduced pressure atmosphere at high altitude in Tibet, *FUEL*, 2013;
338 111:298-304. <https://doi.org/10.1016/j.fuel.2013.04.032>
- 339 [10] R Tu, J Fang, YM Zhang, J Zhang, Y Zeng. Effects of low air pressure on radiation-controlled
340 rectangular ethanol and n-heptane pool fires, *Proc. Combust. Inst.* 2013; 34:2591-2598.
341 <https://doi.org/10.1016/j.proci.2012.06.036>
- 342 [11] F Tang, LH Hu, ZW Qiu, Q Wang. A global model of plume axial temperature profile transition
343 from axisymmetric to line-source pool fires in normal and reduced pressures, *FUEL*,
344 2014;130:211-214. <https://doi.org/10.1016/j.fuel.2014.04.053>
- 345 [12] XC Zhang, LH Hu, W Zhu, XL Zhang, LZ Yang. Axial temperature profile in buoyant plume
346 of rectangular source fuel jet fire in normal- and a sub-atmospheric pressure, *FUEL*, 2014;134:455-
347 459. <https://doi.org/10.1016/j.fuel.2014.05.046>
- 348 [13] F Tang, KJ Zhu, MS Dong, Q Shi. Mean flame height and radiative heat flux characteristic of
349 medium scale rectangular thermal buoyancy source with different aspect ratios in a sub-
350 atmospheric pressure, *Int. J. Heat Mass Transf.* 2015;84:427-432.
351 <https://doi.org/10.1016/j.ijheatmasstransfer.2015.01.037>

- 352 [14] LH Hu, XC Zhang, XL Zhang, KH Lu, ZM Guo. Flame heights and fraction of stoichiometric
353 air entrained for rectangular turbulent jet fires in a sub-atmospheric pressure, *Proc. Combust. Inst.*
354 2017; 36:2995-3002. <https://doi.org/10.1016/j.proci.2016.07.090>
- 355 [15] J Fang, R Tu, J Guan, et al. Influence of low air pressure on combustion characteristics and
356 flame pulsation of pool fires, *FUEL*, 2011; 90:2760-2766.
357 <https://doi.org/10.1016/j.fuel.2011.03.035>
- 358 [16] NA Liu, SJ Zhang, XS Luo, J Lei, HX Chen, XD Xie, LH Zhang, R Tu. Interaction of two
359 parallel rectangular fires, *Proc. Combust. Inst.* 2019; 37:3833-3841.
360 <https://doi.org/10.1016/j.proci.2018.06.158>
- 361 [17] PX He, P Wang, K Wang, XP Liu, CM Wang, CF Tao, YQ Liu. The evolution of flame height
362 and air flow for double rectangular pool fires, *FUEL*, 2019; 237:486-493.
363 <https://doi.org/10.1016/j.fuel.2018.10.027>
- 364 [18] F Tang, ZL Cao, A Palacios, Q Wang. A study on the maximum temperature of ceiling jet
365 induced by rectangular-source fires in a tunnel using ceiling smoke extraction, *Int. J. Therm. Sci.*
366 <https://doi.org/10.1016/j.ijthermalsci.2018.02.001>
- 367 [19] J Ji, YY Fu, CG Fan, et al. An experimental investigation on thermal characteristics of sidewall
368 fires in corridor-like structures with varying width, *Int. J. Heat Mass Transf.* 2015; 84:562-570.
369 <https://doi.org/10.1016/j.ijheatmasstransfer.2015.01.020>
- 370 [20] J Ji, TT Tan, ZH Gao, KY Li. Influence of sidewall and aspect ratio on burning behavior of
371 rectangular ethanol and heptane pool fires, *Fuel*, 2019;238:166-172.
372 <https://doi.org/10.1016/j.fuel.2018.10.112>

- 373 [21] XL Zhang, LH Hu, MA Delichatsios, JP Zhang. Experimental study on flame morphologic
374 characteristics of wall attached non-premixed buoyancy driven turbulent flames, *Applied Energy*,
375 2019; 254:113672. <https://doi.org/10.1016/j.apenergy.2019.113672>
- 376 [22] EE Zukoski, T Kubota, B Cetegen. Entrainment in Fire Plumes, *Fire Saf. J.* 1980; 81:107-121.
377 [https://doi.org/10.1016/0379-7112\(81\)90037-0](https://doi.org/10.1016/0379-7112(81)90037-0)
- 378 [23] Y Hasemi, T Tokunaga. Some Experimental Aspects of turbulent diffusion flames and buoyant
379 plumes from fire sources against a wall and in a corner of walls, *Combust. Sci. Technol.* 1984;
380 40:1-17. <https://doi.org/10.1080/00102208408923795>
- 381 [24] M Poreh, G Garrad. A study of wall and corner fire plumes, *Fire Saf. J.* 2000; 34:81-98.
382 [https://doi.org/10.1016/S0379-7112\(99\)00040-5](https://doi.org/10.1016/S0379-7112(99)00040-5)
- 383 [25] CG Fan, J Ji, YZ Li, H Ingason, JH Sun. Experimental study of sidewall effect on flame
384 characteristics of heptane pool fires with different aspect ratios and orientations in a channel, *Proc.*
385 *Combust. Inst.* 2017; 36:3121-3129. <https://doi.org/10.1016/j.proci.2016.06.196>
- 386 [26] ZH Gao, ZX Liu, J Ji, CG Fan, LJ Li, JH Sun. Experimental study of tunnel sidewall effect on
387 flame characteristics and air entrainment factor of methanol pool fires, *Appl. Therm. Eng.* 2016;
388 102:1314-1319. <https://doi.org/10.1016/j.applthermaleng.2016.03.025>
- 389 [27] X Huang, Y Wang, H Zhu, L He, F Tang, J Wen. Experimental study on the radiant heat flux
390 of wall-attached fire plume generated by rectangular sources, *Int. J. Therm. Sci.* 2020;159:106605.
391 <https://doi.org/10.1016/j.ijthermalsci.2020.106605>
- 392 [28] LH Hu, SX Liu, XL Zhang. Flame heights of line-source buoyant turbulent non-premixed jets
393 with air entrainment constraint by two parallel side walls, *FUEL*, 2017; 200:583-589.
394 <https://doi.org/10.1016/j.fuel.2017.03.082>

- 395 [29] XL Zhang, LH Hu, M.A. Delichastios, JP Zhang. Experimental study and analysis on flame
396 lengths induced by wall-attached fire impinging upon an inclined ceiling, *Proc. Combust. Inst.*
397 2019; 37:3879-3887 <https://doi.org/10.1016/j.proci.2018.06.203>
- 398 [30] CF Tao, Y Shen, RW Zong, F Tang. An experimental study of flame height and air entrainment
399 of buoyancy controlled jet flames with sidewalls, *FUEL*, 2016; 183:164-169.
400 <https://doi.org/10.1016/j.fuel.2016.06.054>
- 401 [31] F Tang, P Hu, J Zhang, J Wen. Heat fluxes under the ceiling induced by wall fires with various
402 burner aspect ratios in a channel, *Proc. Combust. Inst.* 2020,
403 <https://doi.org/10.1016/j.proci.2020.05.029>
- 404 [32] F Tang, P Hu, J Wen. Experimental investigation on lateral ceiling temperature distribution
405 induced by wall-attached fire with various burner aspect ratios in underground space, *Fire Saf. J.*
406 2020; 3:103055. <https://doi.org/10.1016/j.firesaf.2020.103055>
- 407 [33] J Fang, C Jiang, J Wang, et al. Oscillation frequency of buoyant diffusion flame in cross-wind,
408 *FUEL*, 2016; 15:856-863. <https://doi.org/10.1016/j.fuel.2016.07.084>
- 409 [34] DP Kong, Zhen Zhang, P Ping, et al. Experimental study on burning behavior of crude oil pool
410 fire in annular ice cavities, *FUEL*, 2018; 15:464-472.
411 <https://doi.org/10.1016/j.fuel.2018.07.049>
- 412 [35] WMG Malalasekera, HK Versteeg, K Gilchrist. A review of research and an experimental
413 study on the pulsation of buoyant diffusion flames and pool fires, *Fire Mater.*, 1996; 20:261-271.
414 [https://doi.org/10.1002/\(SICI\)1099-1018\(199611\)20:6<261::AID-FAM578>3.0.CO;2-M](https://doi.org/10.1002/(SICI)1099-1018(199611)20:6<261::AID-FAM578>3.0.CO;2-M)
- 415 [36] BM Cetegen, TA Ahmed. Experiments on periodic instability of buoyant plumes and pool fires,
416 *Combust. Flame.* 1993; 93:157-184. [https://doi.org/10.1016/0010-2180\(93\)90090-P](https://doi.org/10.1016/0010-2180(93)90090-P)

- 417 [37] BJ McCaffrey. Fire plume dynamics – A review presented at the conference on large-scale fire
418 phenomenology, NBS, Gaithersburg, MD, 1984:10-13
- 419 [38] XL Zhang, X Fang, YL Miao, et al. Experimental study on pulsation of free-, wall-, corner
420 buoyant turbulent diffusion flames, *FUEL*, 2020; 276:118022.
421 <https://doi.org/10.1016/j.fuel.2020.118022>
- 422 [39] BM Cetegen, Y Dong, MC Soteriou. Experiments on stability and oscillatory behavior of
423 planar buoyant plumes, *Phys. Fluids.*, 1998; 10:1658-1665. <https://doi.org/10.1063/1.869683>
- 424 [40] F Tang, LH Hu, Q Wang, ZJ Ding. Flame pulsation frequency of conduction-controlled
425 rectangular hydrocarbon pool fires of different aspect ratios in a sub-atmospheric, *Int. J. Heat Mass.*
426 *Transf.* 2014; 76:447-451. <https://doi.org/10.1016/j.ijheatmasstransfer.2014.04.047>
- 427 [41] EJ Weckman, AB Strong. Experimental investigation of the turbulence structure of medium-
428 scale methanol pool fire, *Combust. Flame.* 1996; 105:243-266. [https://doi.org/10.1016/0010-
429 2180\(95\)00103-4](https://doi.org/10.1016/0010-2180(95)00103-4)
- 430 [42] D Zeinali, S Verstockt, T Beji et al. Experimental study of corner fires – Part I: Inert panel tests,
431 *Combust. Flame.* 2018; 189:472-490. <https://doi.org/10.1016/j.combustflame.2017.09.034>

432